

VALIDATED MODEL OF A PRESSURE MICROPROBE FOR WATER RELATIONS OF PLANT CELLS

Victor Bertucci-Neto and Paulo Estevão Cruvinel

Embrapa Instrumentação Agropecuária, Rua XV de Novembro, 1452, 13560-970, São Carlos, SP, Brazil

Keywords: Model vegetable cell, Pressure probe, Instrument turgor.

Abstract: Turgor pressure is a physiologic variable of fundamental importance. It is a component of water potential and a measure of water status in a plant. For a long time direct measurement of turgor pressure was not possible. Three decades ago a pressure probe technique was originally introduced to measure turgor pressure and water relations of higher plant cells. Early experiments were made with a glass capillary linked to a pressure chamber, filled with silicone oil. After the vegetable cell to be punctured with the tip of the capillary, a sensor was used to measure the pressure in the chamber. From then until now the usual procedure has been to detect the meniscus position at the moment that the cell is punctured and manually, or automatically, to return the meniscus to the original position. When this occurs the pressure in the chamber is measured with a sensor. Some attempts were made to get the instrument automated but there is no systematic description about it. Based on this, it is proposed a dynamic model for the hydraulic system that can be helpful to design a closed loop system aiming an automated instrument. It is also shown that the theoretical model reasonably matches the experimental results.

1 INTRODUCTION

Turgor pressure is a physiologic variable of fundamental importance. It is a component of water potential and a measure of water status in a plant. For mature, turgid cells of higher plants, changes of water potential are largely reflected in changes of turgor. For a long time, the direct measurement of turgor was not possible (Steudle, 1993). Three decades ago a pressure probe technique was originally introduced to measure turgor and water relations of higher plant cells (Husken *et al.*, 1978). Early experiments were made with a glass capillary linked to a pressure chamber, filled with silicone oil. After the vegetable cell to be punctured with the tip of the capillary, a sensor was used to measure the pressure in the chamber. Later, it was remarked that a necessary condition for constructing cell pressure probes is given by:

$$\frac{V_{ol}}{B} \gg c_{ol} V_{in} \quad (1)$$

where V_{ol} and V_{in} are the internal volumes of the cell and apparatus respectively, B is the elastic

coefficient of the cell, and c_{ol} is the coefficient of compressibility of the oil. The condition imposed by

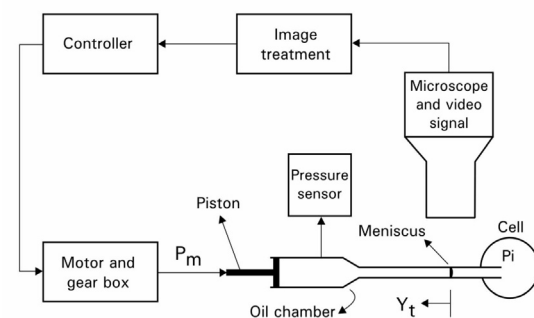


Figure 1: Schematic diagram of a pressure microprobe.

Equation (1) indicates that V_{in} must be reduced in several orders of magnitude, and the meniscus formed at the tip of the capillary must be used as a reference of measurement. From then to now the usual procedure has been to detect the meniscus position at the moment that the cell is punctured manually, or automatically, to return the meniscus to the original position. When this occurs the pressure in the chamber is measured with a sensor. In the Figure 1 is shown a schematic diagram representing

the pressure probe acting on a cell, with the meniscus being observed by the microscope and video camera. After the image treatment, the signal equivalent to the meniscus position is sent to the controller. The controller acts on the motor and reducing gear causing the movement of the piston returning the meniscus to the original position. Some attempts were made to get the instrument automated (Husken *et al.*, 1978, and Cosgrove and Durachko, 1986) but there is no systematic description about it. Manual measurements can be made during short times but it can be difficult if one wants to register long term behaviour. Moreover, manual operation is based on the operator skill and in the subjective interpretation of the image. By the other hand, control system algorithms can be more easily designed and implemented when the system plant is reasonably known. Based on this, it is proposed a dynamic model for the hydraulic system that can be helpful to design a closed loop system aiming an automated instrument. In addition, the mathematical model can be useful to understand the contribution of each physical parameter to the measurement performance.

2 SYSTEM MODELLING

The system modelling is based on the analysis of pipe flow. It is considered a cylindrical element (radius= r , and length= L) in a pipeline and expressed the loss in pressure due to the forces acting on the fluid. Balancing the forces in terms of the pressure p along the longitudinal axis y , including the retarding force due to the shear stress τ_w gives:

$$[p - (p + dp)] (\pi r^2) = \tau_w (2\pi r) dy \quad (2)$$

resulting in:

$$-dp = \frac{2\tau_w}{r} dy \quad (3)$$

Integrating both sides of Equation (3) from the pressure at the downstream end to the upstream end, and along the length of the element, yields the amount in pressure Δp that dropped:

$$\Delta p = \frac{2\tau_w}{r} L \quad (4)$$

Last equation shows the relation between shear stress and the pressure drop. Δp can be equated to the specific weight $\gamma = \rho g$ (density multiplied by

gravity acceleration) multiplied by the heading loss h_L . Then Equation (4) can be rewritten:

$$\tau_w = \frac{\gamma h_L}{2L} r \quad (5)$$

In the case of laminar flow in the pipe Newton's law of viscosity can be written as τ_w being proportional to the velocity gradient v related to the radius, with constant of proportionality defined as the coefficient of viscosity μ . Then Equation (5) can be written:

$$\tau_w = \frac{\gamma h_L}{2L} r = -\mu \frac{dv}{dr} \quad (6)$$

Integrating last equation from the maximum velocity v_c (at the center of the pipe) to v , and from 0 to r , becomes:

$$v = v_c - \frac{\gamma h_L}{4\mu L} r^2 \quad (7)$$

Last equation shows that the velocity profile is a parabolic curve. When $r=0$, $v=v_c$. Substituting $v=0$, and $r=d_t/2$ (d_t is the tube diameter), and considering $v_c = 2V$, being V the mean velocity, then:

$$h_L = \frac{32\mu LV}{\gamma d_t^2} \quad (8)$$

showing that the head loss is proportional to the mean velocity. By setting Equation (8) equal to Darcy's equation (Vennard, 1961) it can be derived an expression for the friction factor for laminar pipe flow:

$$f = \frac{64\mu}{V d_t \rho} \quad (9)$$

By the other hand, multiplying both sides of Darcy's equation by $\gamma = \rho g$ and equating to the same pressure drop $h_L \gamma$ obtained in Equation (5):

$$\Delta p = h_L \gamma = f \rho \frac{L}{d_t} \frac{V^2}{2} = \tau_w \frac{4L}{d_t} \Rightarrow \tau_w = f \rho \frac{V^2}{8} \quad (10)$$

Using the friction factor given in the Equation (9) and substituting in the last equation it is obtained an expression that relates the shear stress to the velocity, or:

$$\tau_w = \frac{8\mu V}{d_t} \quad (11)$$

The analysis that follows is described in Doebelin (1990) that considered a gas system with tube

volume a small fraction of chamber volume. However the flow considered here is liquid causing a simplification because the spring effect that exists due to the gas flow is negligible in liquid flow case. Analysis consists of applying Newton's law by balancing the forces along the tube in the longitudinal axis y . Initially is considered that $p_m=p_i=p_0$ (p_0 an initial arbitrary value) when p_i changes slightly in some way. Then it is considered at this point that p_i and p_m mean the excess pressures over and above p_0 . The force f_i due to the pressure p_i is given by:

$$f_i = p_i A = \frac{\pi d_t^2}{4} p_i \quad (12)$$

The viscous force f_v due to the wall shearing stress is given by the division of Equation (11) by the area of the pipe wall:

$$f_v = 8\pi\mu L \dot{V} = 8\pi\mu L \dot{y}_t \quad (13)$$

where y_t is the liquid displacement due to p_i action. This displacement causes a volume change $dV_{ol}=\pi d_t^2 y_t/4$ and pressure excess $p_m=\pi B d_t^2 y_t/(4V_{ol})$ (B is the elastic coefficient). The equivalent force is given by:

$$f_m = \frac{\pi^2 B d_t^4 y_t}{16V_{ol}} \quad (14)$$

Applying Newton's law along the longitudinal axis implies to balance the forces and equate to the fluid mass m multiplied by the acceleration a , or:

$$f_i - f_v - f_m = m \cdot a \quad (15)$$

Above equation is useful for uniform velocity distribution. However, the quadratic velocity profile verified in Equation (7) indicates that a correction factor must be used in the right side of Equation (15). In this case the quantity $m \cdot a$ must be multiplied by $4/3$. Then, Equation (15) can be rewritten as:

$$\frac{\pi d_t^2}{4} p_i - 8\pi\mu L \dot{y}_t - \frac{\pi^2 B d_t^4}{16V_{ol}} y_t = \frac{\pi d_t^2 L \rho}{3} \ddot{y}_t \quad (16)$$

Applying Laplace transform in Equation (16) yields:

$$G_{yp}(s) = \frac{Y_t(s)}{P_i(s)} = \frac{\frac{3}{4L\rho}}{s^2 + \frac{24\mu}{\rho d_t^2} s + \frac{3\pi B d_t^2}{16L\rho V_{ol}}} \quad (17)$$

Last equation relates the displacement of the

meniscus due to the pressure applied at the tip of the capillary. Moreover, it permits an evaluation of the dynamical behaviour by the variation of its physical parameters.

3 EXPERIMENTAL SET UP AND COMPARISON

The meniscus was observed with a video camera coupled to a microscope. The video signal was sampled at 70 ms and digitalized with a video board installed in the personal computer. It was developed a software based on *Imaq Vision* for *LabView* for the meniscus detection. This software is based on pattern recognition and gives as result the number of pixels (Npixel) concerning to the previously chosen initial position. It was coupled a "T" connection at the tip of the capillary. The capillary was previously filled with silicone oil. It was linked at one of the inputs of the T connection an air duct supplied by an air compressor. At the other input was coupled a pressure sensor with reading rate equal to 10mV/psi. After the air compressor to be switched on, the readings of both meniscus position, and voltage signal due to the sensor were collected and stored in the computer. In the Figure 2 is shown the curve due to the meniscus displacement (in Npixel) and the curve due to the voltage signal in the pressure sensor. It can be seen in Equation (17) that the final value is L/B . This means that if the length L is increased then the meniscus displacement is also increased. It was used the following values for each physical parameter in the Equation (17), with B , μ , and ρ being attributed to the silicone oil, and L chosen according to the optical resolution: $L=0.15\text{m}$; $d_t=270 \cdot 10^{-6} \text{ m}$; $\rho=900 \text{ Kg/m}^3$; $B=2.18 \cdot 10^9 \text{ N/m}^2$; $\mu=10^{-3} \text{ Kg/m s}$. Substituting the above values results in:

$$G_{yp}(s) = \frac{5.556 \cdot 10^{-6}}{s^2 + 365.8 \cdot s + 8.074 \cdot 10^7} \quad (18)$$

To compare the mathematical model to the experimental response it is necessary to transform the pressure sensor signal measured in volt in pressure dimension. Then, the voltage signal must be multiplied by $(1/0.6\text{mV}) \times \text{psi}$, with $1\text{psi}=6894.6 \text{ N/m}^2$. The relation between the meniscus displacement in meter and Npixel was previously measured with a rule adapted in the microscope lens. It was found $1 \text{ pixel}=1/6.36 \times 10^5 \text{ m}$. Applying the transformed input pressure signal to the Equation

(18) results in the red curve showed in Figure 3. This same figure shows the experimental curve.

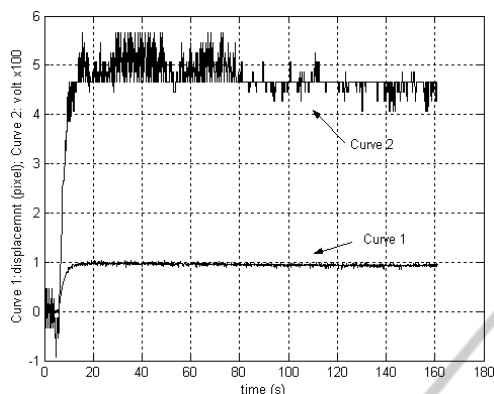


Figure 2: Curve 1: meniscus displacement (Npixel). Curve 2: pressure sensor signal (volt x 100).

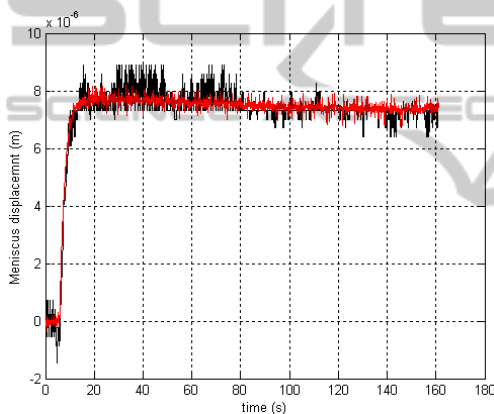


Figure 3: Meniscus displacement: experimental response (black), and theoretical response (red).

4 CONCLUSIONS

Despite the noisy signal imposed by the meniscus detection (mean=0.47 Npixel and variance=0.10 Npixel²) it can be seen in Figure 3 the strong accordance between the theoretical and experimental responses. The mathematical model could match the dynamical behaviour and the steady state exhibited in the experimental response. It was not considered in the modelling the effects of the surface tension and the glass compressibility because the magnitude of both of them were previously known as negligible. Experimental results show that the proposed model can be applied in open and closed loop designs according to the operation needs (manual or automated). The modelling is also justified in the evaluation of the contribution of each

physical parameter to the system response. This permits to predict the importance of using high or low viscosity silicone oil, a long or short pipe, or the more or less compressible oil. All of these considerations will be related to the system range and performance.

ACKNOWLEDGEMENTS

This work was supported by Embrapa.

REFERENCES

- Bertucci-Neto, V. 2005. Modelagem e automação em nova técnica de medida para relações de água e planta. Thesis (in portuguese). Escola de Engenharia de São Carlos, Universidade de São Paulo. São Carlos.
- Cosgrove, D. J.; Durachko, D. M. 1986. Automated pressure probe for measurement of water transport properties of higher plant cells. *Review of Scientific Instrument.* v.57. n.10. p.2614-2619.
- Doebelin, E. O. 1990. Measurement systems application and design. 4. ed. New York: McGraw-Hill Publishing Company.
- Husken, D.; Steudle, E.; Zimmermann, U. 1978. Pressure probe technique for measuring water relations of cells in higher plants. *Plant Physiology.* v. 61. p. 158-163.
- Steudle, E. 1993. Pressure probe technique: basic principles and application to studies of water and solute relations at the cell, tissue and organ level. Ed. J. A. C. Smith and H. Griffiths. Oxford, UK: Bios Scientific Publishers Ltd. p.5-36.
- Vennard, J. K. (1961). Elementary fluid dynamics. 4. ed. New York: John Wiley and Sons, Inc.